Opposing Roles of JNK and p38 in Lymphangiogenesis in Melanoma

Emmi Puujalka[1], Magdalena Heinz[1], Bastian Hoesel[2], Peter Friedl[1], Bernhard Schweighofer[1], Judith Wenzina[1], Christine Pirker[3], Johannes A. Schmid[2], Robert Loewe[1], Erwin F. Wagner[4], Walter Berger[3] and Peter Petzelbauer[1]

In primary melanoma, the amount of vascular endothelial growth factor C (VEGF-C) expression and lymphangiogenesis predicts the probability of metastasis to sentinel nodes, but conditions boosting VEGF-C expression in melanoma are poorly characterized. By comparative mRNA expression analysis of a set of 22 human melanoma cell lines, we found a striking negative correlation between VEGF-C and microphthalmia-associated transcription factor (MITF) expression, which was confirmed by data mining in GEO databases of human melanoma Affymetrix arrays. Moreover, in human patients, high VEGF-C and low MITF levels in primary melanoma significantly correlated with the chance of metastasis. Pathway analysis disclosed the respective c-Jun N-terminal kinase and p38/mitogen-activated protein kinase activities as being responsible for the inverse regulation of VEGF-C and MITF. Predominant c-Jun N-terminal kinase signaling results in a VEGF-C^{low}/MITF^{high} phenotype; these melanoma cells are highly proliferative, show low mobility, and are poorly lymphangiogenic. Predominant p38 signaling results in a VEGF-C^{high}/MITF^{low} phenotype, corresponding to a slowly cycling, highly mobile, lymphangiogenic, and metastatic melanoma. In conclusion, the relative c-Jun N-terminal kinase and p38 activities determine the biological behavior of melanoma. VEGF-C and MITF levels serve as surrogate markers for the respective c-Jun N-terminal kinase and p38 activities and may be used to predict the risk of metastasis in primary melanoma.

INTRODUCTION

Most solid primary tumors induce lymphangiogenesis and use the lymphatic network to seed to distant sites (Podgrabinska and Skobe, 2014; Stacker et al., 2014). Among skin tumors, melanoma is the most efficient in inducing lymphangiogenesis (Shields et al., 2004). Even thin lesions may metastasize (Balch et al., 2009) and number of tumor-associated lymphatic vessels clearly correlate with the risk for metastasis (Dadras et al., 2003; Pastushenko et al., 2014).

Vascular endothelial growth factor C (VEGF-C) is the most potent inducer of lymphangiogenesis (Jeltsch et al., 1997). Inhibition of lymphangiogenesis by blockade of VEGF-C or its receptor VEGFR-3 prevents lymph node metastases in animal models without affecting primary tumor growth (Podgrabinska and Skobe, 2014). Also in human cancer, VEGF-C expression was found to correlate with metastasis (Cianfarani et al., 2012; Doeden et al., 2009; Schietroma et al., 2003).

Transcriptional regulation of VEGF-C gene involves PI3K-Akt, extracellular signal-regulated kinase 1/2, NFκB, and p38 pathways (Chen et al., 2013; Luangdilok et al., 2011). In melanoma, Wnt1 (Niederleithner et al., 2012), EGF (Bracher et al., 2013), and the met proto-oncogene (Swoboda et al., 2012) regulate VEGF-C expression, but a profound understanding for the heterogeneity of VEGF-C expression in melanoma is missing. Characterization of pathways regulating VEGF-C expression may define markers in primary melanoma for predicting metastasis, thereby avoiding sentinel node biopsy. Moreover, it may specify novel targets for adjuvant treatment for advanced melanoma as there is evidence that inhibition of lymphangiogenesis by blocking VEGFR-3 in combination with VEGFR-2 diminishes distant metastasis in animal models (Matsui et al., 2008; Roberts et al., 2006).

Microphthalmia-associated transcription factor (MITF) is a key protein involved in melanocyte-specific pathway regulation (Mort et al., 2015). In melanoma, expression levels are highly heterogeneous. High expression results in melanocyte differentiation, intermediate levels in proliferation, and low levels in an invasive cell phenotype. The amount of MITF expression is at least partially responsible for a phenomenon called "phenotype switching," which describes the difference between tumor cells growing locally with poor metastatic potential and cells that have acquired a slow proliferating, stem cell-like phenotype with high invasive potential

[1]Department of Dermatology, Skin and Endothelium Research Division (SERD), Medical University of Vienna, Austria; [2]Department of Vascular Biology and Thrombosis Research, Center for Physiology and Pharmacology, Medical University of Vienna, Austria; [3]Department of Medicine I, Institute of Cancer Research and Comprehensive Cancer Center, Medical University of Vienna, Austria; and [4]BBVA Foundation-CNIO Cancer Cell Biology Program, Spanish National Cancer Research Centre (CNIO), Madrid, Spain

Correspondence: Peter Petzelbauer, Skin and Endothelium Research Division (SERD), Department of Dermatology, Medical University of Vienna, Austria E-mail: peter.petzelbauer@meduniwien.ac.at

(Carreira et al., 2006; Cheli et al., 2012; Hoek and Goding, 2010; Koludrovic and Davidson, 2013).

On the basis of mRNA expression arrays from 22 human melanoma lines, we found a striking negative correlation between expression of VEGF-C and MITF in human melanoma cell lines. These data were confirmed by GEO database screening and by immunohistochemistry from human samples. Here we describe how the inverse expression pattern of VEGF-C and MITF in melanoma is under the control of c-Jun N-terminal kinase (JNK) and p38-mitogen-activated protein kinase (MAPK) signaling pathways.

RESULTS

Negative correlation between VEGF-C and MITF in cell lines and clinical samples

To understand mechanisms underlying the wide range of constitutively expressed VEGF-C levels in 22 human melanoma cell lines (Supplementary Figure S1a online), Pearson correlation analysis of Agilent microarray mRNA data was performed (probe IDs in Supplementary Figure S1b) revealing a single best negative correlation of VEGF-C with MITF (Figure 1a). Also genes involved in MITF regulation and MITF target genes (Hartman and Czyz, 2015; Hoek et al., 2008a, 2008b; Howlin et al., 2015) negatively correlated with VEGF-C and positively with MITF (Supplementary Table S1 online). The BRAF and NRAS status as well as the origin of cell lines did not correlate with VEGF-C or MITF levels (Supplementary Figure S1d). The negative correlation between VEGF-C and MITF mRNA expression was confirmed in Affymetrix arrays from the GEO database analyzing human melanoma samples (11 datasets, Figure 1b; the corresponding scatter plots are presented in Supplementary Figure S1f).

Next, VEGF-C and MITF protein expression levels were semiquantitatively analyzed in human melanoma metastasis samples (n = 103) by immunohistochemistry and staining intensities were scored on a scale 1–3 (exemplified in Figure 1c). Results exhibit that MITF protein expression negatively correlates with VEGF-C protein expression (Figure 1d). IgG isotype controls for antibodies and positive controls (A375 cells overexpressing VEGF-C) are shown in Supplementary Figure S1e.

Finally, VEGF-C and MITF protein expression levels were semiquantitatively analyzed in a retrospective study from human primary melanoma samples diagnosed between 2008 and 2010. Patients without subsequent metastasis (n = 22; age 65 + 16 years, Breslow 2 + 1.7 mm) had a documented tumor-free follow-up of 5.5 + 1 years. In patients with metastasis (n = 9; age 69 + 10 years, Breslow 5.7 + 5.2 mm), the interval between excision and metastasis was 3 + 3.7 months. Patients with metastasis had significantly higher VEGF-C and lower MITF expression levels in primary lesions compared with the patients without metastasis (Figure 1e).

Thus, these four independent approaches consistently establish the negative correlation of MITF and VEGF-C mRNA and protein expression.

The JNK pathway determines VEGF-C and MITF expression levels in melanoma

To understand regulatory mechanisms of VEGF-C and MITF, Agilent microarray mRNA data were subjected to pathway analysis. We found a negative correlation between JNK/MAPK pathway target genes with VEGF-C and a positive correlation with MITF. In contrast, p38/MAPK targets, negative regulators of JNK/MAPK activity, and NFκB targets positively correlated with VEGF-C and negatively with MITF mRNA expression. A positive correlation with VEGF-C was also found for VEGF-C cleavage genes and with matrix metalloproteinases (Supplementary Table S1). For VEGF-C, MITF, sex determining region Y-box 10 (SOX10), and SOX9 genes, the correlation analysis based on microarrays was confirmed by RT-PCR (Supplementary Figure S1c).

Assessing JNK and p38 pathway activities revealed high JNK phosphorylation (p-JNK) in VEGF-C^{low} cells and prominent p38 phosphorylation (p-p38) in VEGF-C^{high} cells (Figure 2a). Expression of total JNK or p38 proteins did not correlate with the VEGF-C expression (Supplementary Figure S2a online). Treatment of cells with specific inhibitors confirmed the regulatory role of these pathways: the JNK inhibitor JNK-IN-8 increased and the p38 inhibitor SB202190 decreased VEGF-C mRNA expression in most of the cell lines (Supplementary Figure S2b and c). The functionality of the inhibitors was confirmed, and the effects were dose dependent (Supplementary Figure S2d–g).

Silencing of JNK1/2 expression in melanoma cells with lentiviral shRNA confirmed the data with JNK-IN-8. The cell lines selected for JNK1/2 silencing were both p-JNK^{high}/p-p38^{low} (VM41) and p-JNK^{low}/p-p38^{high} (VM47 and VM24) (Figure 2a). The knockdown was effective (Figure 3a) and significantly increased VEGF-C mRNA and protein expression (Figure 2b and c) compared with shControl cells. T-5224, which inhibits the JNK downstream target c-Fos (FBJ murine osteosarcoma viral oncogene homolog) (Guinea-Viniegra et al,. 2012), also increased VEGF-C mRNA expression similarly to JNK silencing (Figure 2d). Silencing JNK1 or JNK2 alone did not alter VEGF-C expression (Supplementary Figure S2h). Unexpectedly, overexpression of JNK1/2 did also not change VEGF-C mRNA expression (Supplementary Figure S2i–k), implying that VEGF-C is not directly regulated by the JNK pathway.

Conversely, silencing JNK1/2 significantly decreased MITF mRNA and protein expression, as well as mRNA levels of the MITF upstream regulator SOX10 and the MITF downstream target BCL2A1 (Figure 2e and f) (Hartman and Czyz, 2015). Accordingly, JNK1/2 overexpression increased MITF expression (Supplementary Figure S2i), indicating that the JNK pathway regulates MITF gene transcription. Moreover, the c-Fos inhibitor T-5224 also reduced MITF mRNA expression (Figure 2g). Taken together, JNK1/2 regulates MITF expression by involving c-Fos. Of note, MITF does not regulate VEGF-C expression; overexpression did not alter VEGF-C mRNA or protein levels (Supplementary Figure S2l–o).

VEGF-C expression is upregulated by p38/NFκB

On the basis of the correlation analysis in Supplementary Table S1, we analyzed the effects of the JNK knockdown on p38 and NFκB activities. Silencing of JNK increased phosphorylation of p38, as previously described (Wagner and Nebreda, 2009), and also of p65/NFκB, whereas p44/42 phosphorylation remained unchanged compared with the controls (Figure 3a and b, Supplementary Figure S3a online).
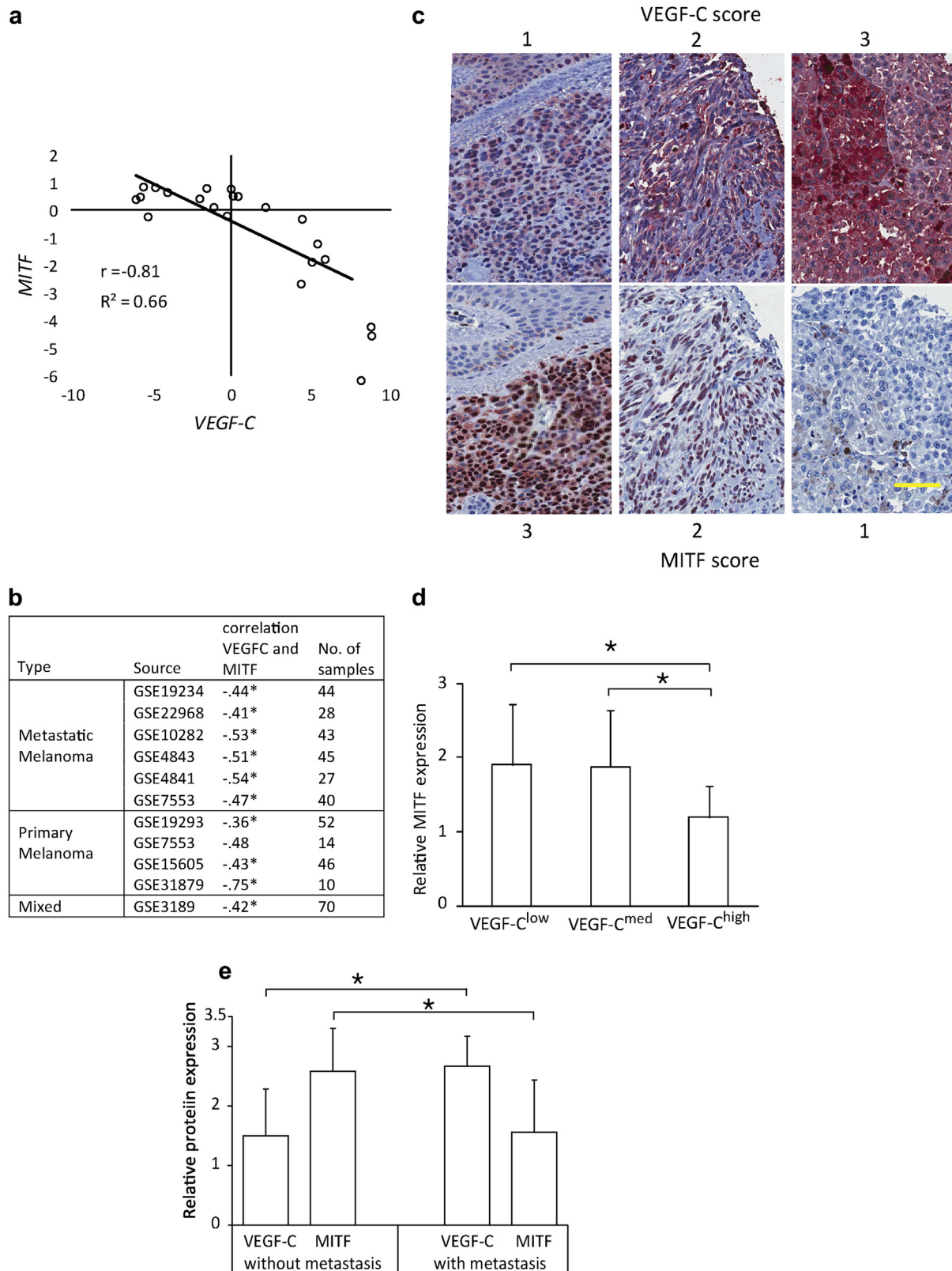
Figure 1. Negative correlation between VEGF-C and MITF expression. (**a**) Fitted regression between MITF and VEGF-C mRNA expression from Agilent arrays in 22 human melanoma cell lines. (**b**) Correlation between VEGF-C and MITF mRNA in Affymerix melanoma arrays from the GEO repository; *$P < 0.05$. (**c**) Examples of IHC-staining scoring of VEGF-C (top) and MITF (bottom) protein expression in serial sections of human melanoma; bar = 100 μm. (**d**) VEGF-C and MITF expression in human melanoma metastasis tissues (n = 103) scored as exemplified in (**c**); *$P < 0.05$, mean ± SD. (**e**) VEGF-C and MITF expression in human primary melanoma tissues (n = 33) scored as exemplified in (**c**). The difference between VEGF-C and MITF expression in primary lesions of patients with (n = 9) and without (n = 24) metastasis during the follow-up is significant; *$P < 0.05$, mean ± SD. IHC, immunohistochemistry; MITF, microphthalmia-associated transcription factor; VEGF-C, vascular endothelial growth factor C.

Figure 2. The ratio of JNK and p38 activities determines VEGF-C and MITF expression levels. (a) Phospho/total protein ratios for JNK and p38 in melanoma lines quantified from western blots (n = 3). Cells are ranked according to VEGF-C expression; mean ± SD. (b) VEGF-C mRNA expression determined by RT-PCR in indicated cells; *P < 0.05, mean ± SD. (c) VEGF-C protein expression assayed by ELISA in indicated cells; *P < 0.05, mean ± SD. (d) VEGF-C mRNA expression determined by RT-PCR in indicated cells with 10 μM c-Fos inhibitor or DMSO for 24 hours; *P < 0.05, mean ± SD. (e) MITF mRNA expression determined by RT-PCR in indicated cells; *P < 0.05, mean ± SD. (f) RT-PCR for indicated MITF pathway genes in indicated cells; mean ± SD. (g) MITF mRNA expression determined by RT-PCR in indicated cells with 10 μM c-Fos inhibitor or DMSO for 24 hours; *P < 0.05, mean ± SD. JNK, c-Jun N-terminal kinase; MITF, microphthalmia-associated transcription factor; VEGF-C, vascular endothelial growth factor C.
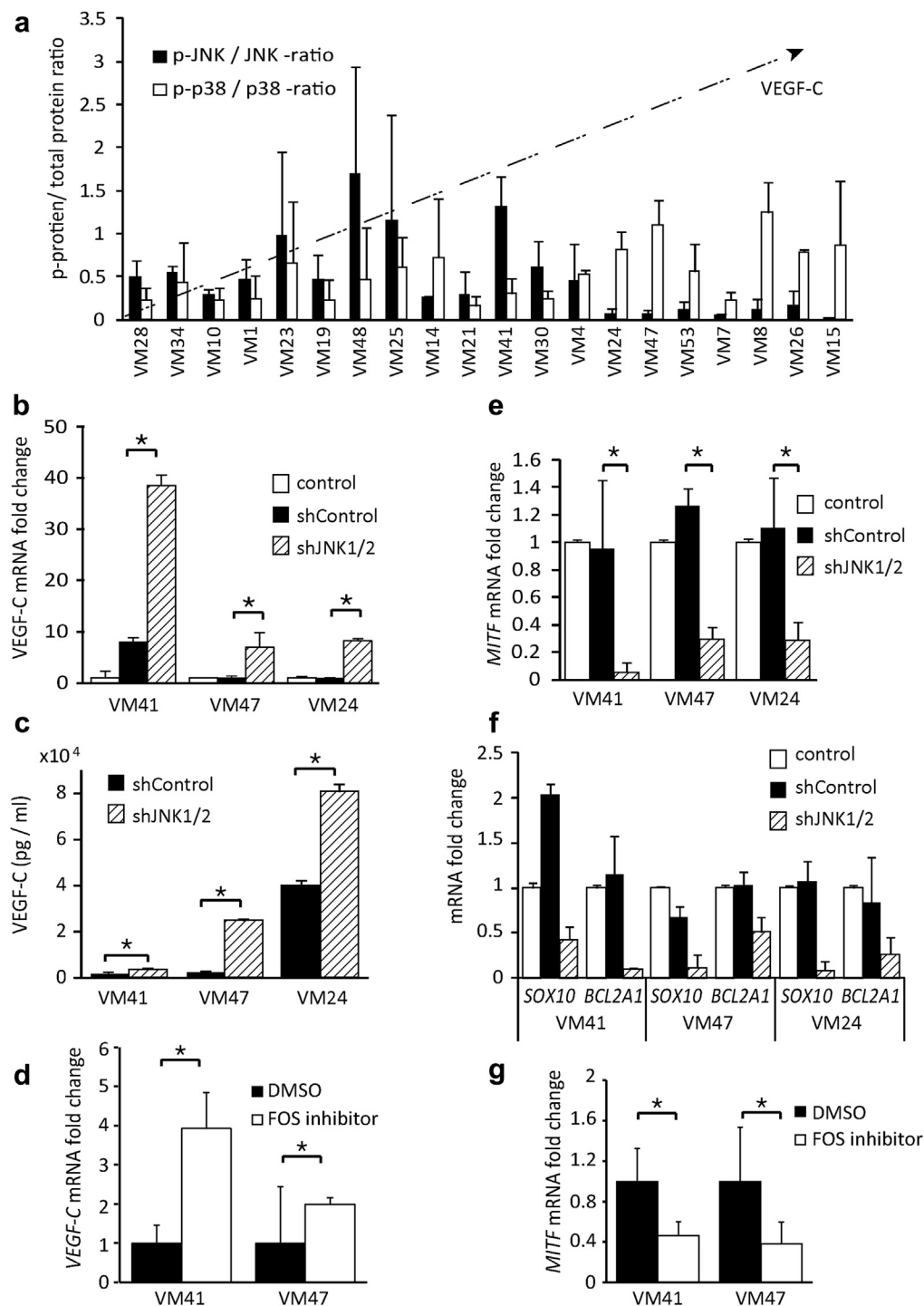
Activation of the p38 pathway by shJNK1/2 or by JNK-IN-8 was confirmed by showing increased mRNA levels of the p38 target SOX9 (Sosa et al., 2014) (Figure 3c, Supplementary Figures S2h and S3b). Of note, over-expression of SOX9 did not change VEGF-C expression (Supplementary Figure S3c and d).

Importantly, JNK silencing not only increased VEGF-C expression, but also the expression of NFκB targets IL6 and IL8 (Figure 3c). Moreover, the expression of these genes was reduced by treating cells with p38 or NFκB inhibitors (Supplementary Figure S3e), supporting the role of p38/NFκB

in their regulation. Also total p65 protein levels follow the pattern of VEGF-C expression in melanoma cells (Supplementary Figure S3f). To confirm the role of NFκB in regulating VEGF-C, we determined the DNA-binding activity of p65 by pulldown (avidin-biotin complex-DNA [ABCD] assay). We found significantly higher p65 binding to oligo-nucleotides carrying the NFκB consensus site, or to oligo-nucleotides containing a stretch of the VEGF-C promoter including the putative NFκB site in shJNK1/2 cells as compared with the shControls (Figure 3d). Appropriate controls are depicted in Figure 3e.
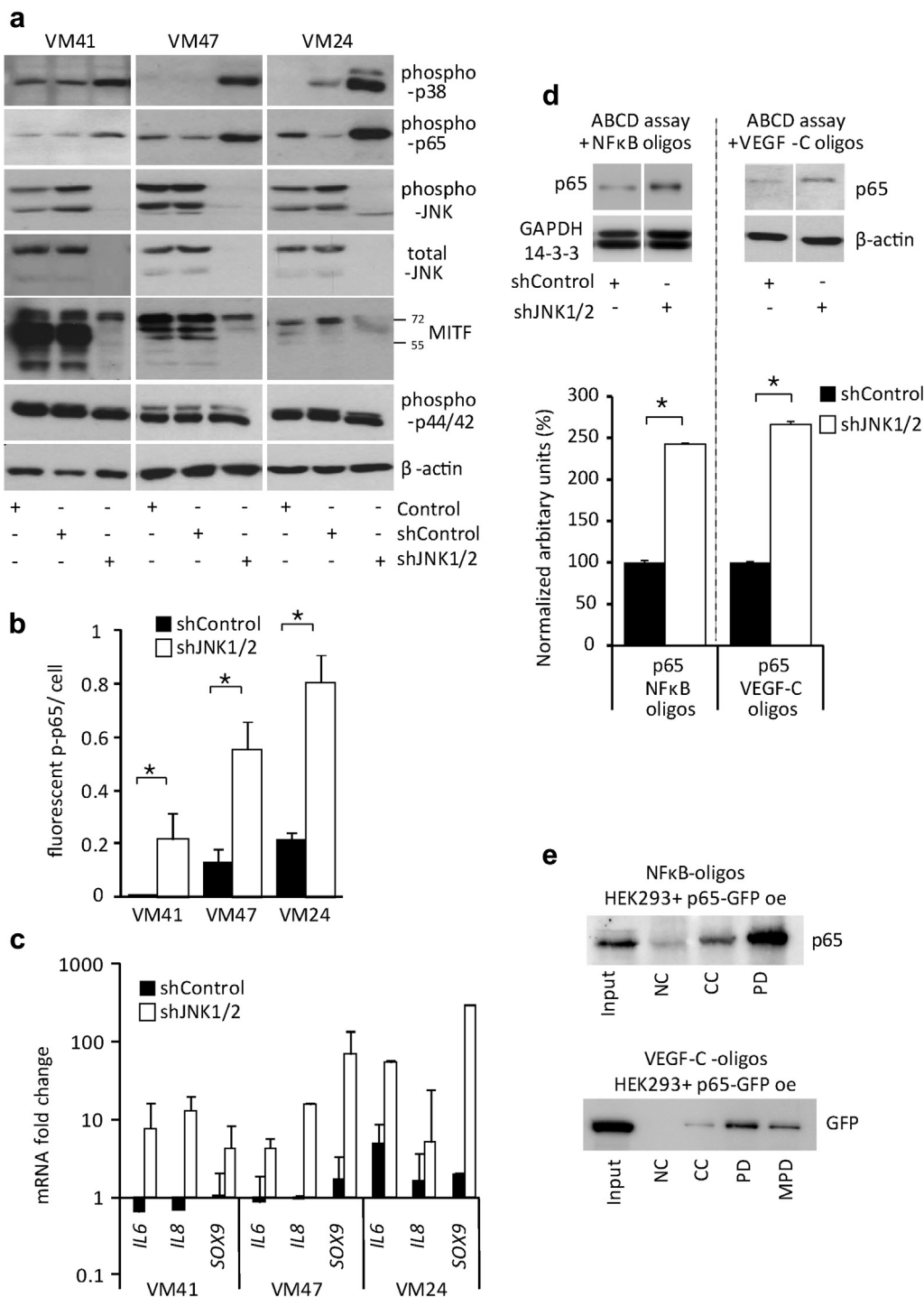
Figure 3. Increased p38 and NFκB activity in shJNK1/2 cells. (a) Representative western blots for indicated proteins in shJNK1/2 and control cells. (b) Quantification of phospho-p65 in shJNK1/2 and control cells by immuno-fluorescence (as exemplified in Supplementary Figure S3a online); $n = 10$/group; *$P < 0.05$, mean ± SD. (c) RT-PCR for p38- (SOX9) and NFκB-pathway targets (IL6, IL8); mean ± SD. (d) DNA-binding activity of p65 by pulldown (ABCD assay) in shJNK1/2 and control samples from VM41 (NFκB oligos) and VM47 (VEGF-C oligos) cells. Top: representative p65 pulldowns with biotinylated oligonucleotides. Bottom: corresponding quantification of bound p65 from the pulldowns; $n = 3$, *$P < 0.05$, mean ± SD. (e) Specificity controls for the ABCD assays with p65/GFP overexpressing HEK293 cells. Top: NFκB consensus. Bottom: NFκB-binding site from the VEGF-C promoter. ABCD, avidin-biotin complex-DNA; CC, cold control; GFP, green fluorescent protein; HEK, human embryonic kidney; Input, cell lysate; JNK, c-Jun N-terminal kinase; MPD, mutated oligonucleotide; NC, no oligonucleotides; PD, biotinylated oligonucleotide, SOX, sex determining region Y; VEGF-C, vascular endothelial growth factor C.

Inhibition of JNK1/2 reduces proliferation but induces an invasive phenotype in vitro

Characterizing the effects of the JNK1/2 knockdown on growth profiles, we found significantly reduced proliferation and reduced entering to the S-cell cycle phase in shJNK1/2 cells (Figure 4a and b, Supplementary Figure S4a online). In contrast, cell migration in a wound healing assay and cell invasion in a Matrigel assay were significantly increased in shJNK1/2 cells (Figure 4c and d, Supplementary Figure S4b). JNK1/2 silencing also caused increased expression of matrix metalloproteinase 7 and/or matrix metalloproteinase 9 mRNA expression (Supplementary Figure S4c). Moreover, supernatants of shJNK1/2 cells induced significantly increased sprouting of human lymphatic endothelial cells in 3D lymphatic endothelial cell-spheroid sprouting assay as compared with spheroids treated with shControl supernatants (Figure 4e and f). Taken together, shJNK1/2 cells are poorly proliferative, but highly invasive and lymphangiogenic in vitro.

**Figure 4. Inhibition of JNK1/2 reduces proliferation but induces an invasive phenotype. (a)** Cell proliferation as determined by the Quant-it PicoGreen method in shJNK1/2 and control cells; mean ± SD. **(b)** Cell cycle analysis as determined by FACS in shJNK1/2 and control cells. **(c)** Cell migration assays quantified as percentage of cell free growth surface area (exemplified in Supplementary Figure S4b online) in shJNK1/2 and control cells; *P < 0.05, mean ± SD. **(d)** Matrigel invasion assays (16 hours) in shJNK1/2 and control cells; *P < 0.05, mean ± SD. **(e)** Quantification of cumulative sprout length (μm) of spheroids composed of lymphatic endothelium treated with supernatants from shJNK1/2 or control VM41 cells. Positive control: supernatants of A375 cells overexpressing VEGF-C; negative control: unconditioned medium; n = 10/group, *P < 0.05, mean ± SD. **(f)** Representative images of spheroids treated with indicated supernatants for 6 hours; original magnification ×20. JNK, c-Jun N-terminal kinase; VEGF-C, vascular endothelial growth factor C.
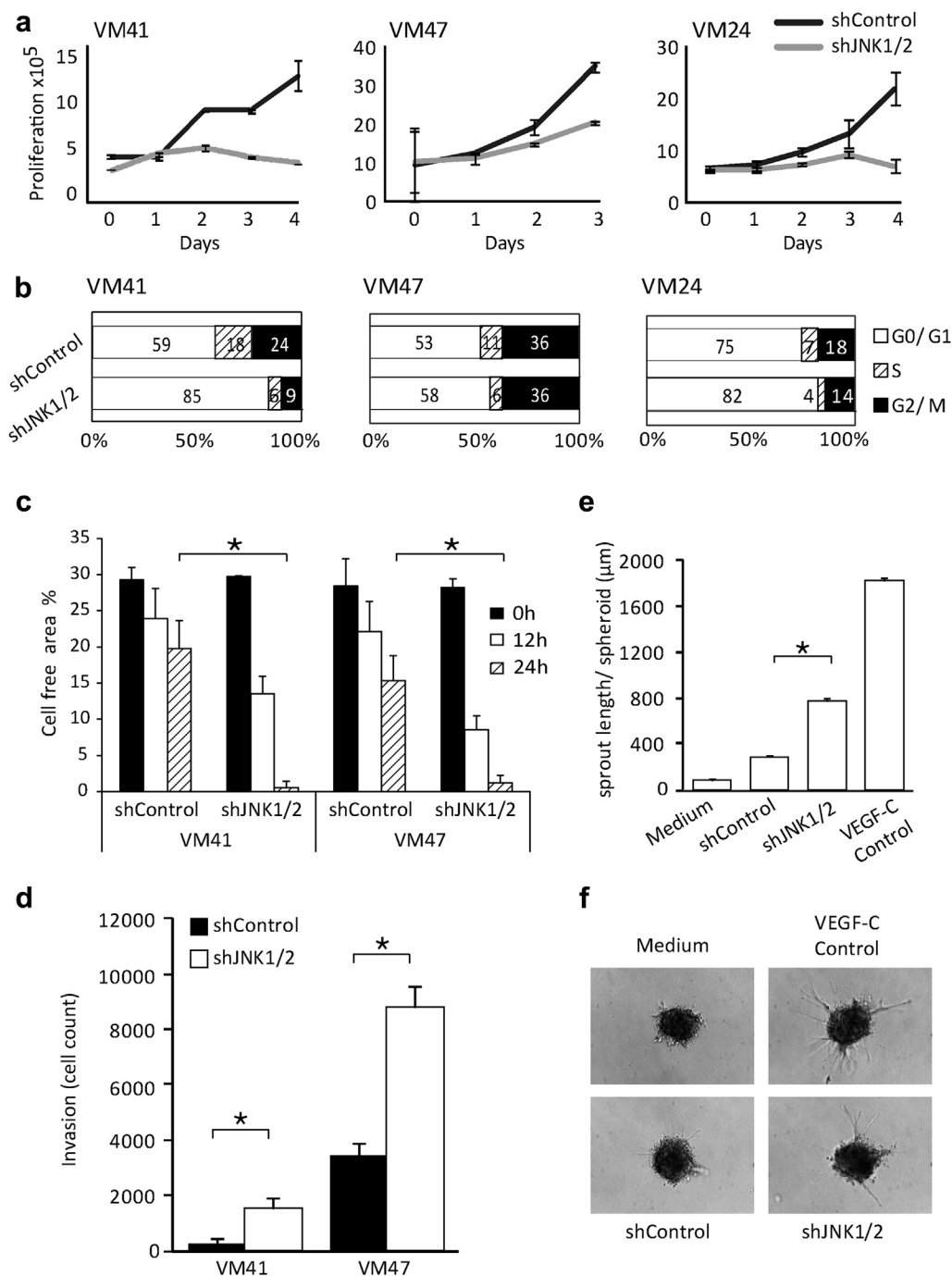
Lymphangiogenic properties of melanomas depend on JNK activity in vivo

To define lymphangiogenic capabilities of melanomas with different p-JNK/p-p38 ratios in vivo, we employed a mouse xenograft and a chicken chorioallantoic *membrane* model. Lymphangiogenesis was quantified by Prox1 (Prospero homeobox protein 1) mRNA expression as a marker for the amount of lymphatic vessels (Niederleithner et al., 2012). In both in vivo models, JNK[high]/p38^{low} cells produced significantly less VEGF-C and had less Prox1 expression, compared with JNK[low]/p38^{high} cells (Figure 5a). There was no correlation between tumor growth and VEGF-C

expression (Supplementary Figure S5a online). We confirmed the relationship between low JNK activity and high lymphangiogenesis in VM41 and VM47 xenografts after JNK1/2 silencing. shJNK1/2 tumors grew slowly and were hardly palpable even after 43 days (Supplementary Figure S5b and c), but even these small tumors showed significantly increased VEGF-C and Prox1 but decreased MITF expression compared with shControls (Figure 5b). On the basis of our results, we propose that the ratio of JNK/p38 activity is responsible for the opposing regulation of VEGF-C and MITF leading to alternative melanoma phenotypes (Figure 5c).

a

b

c
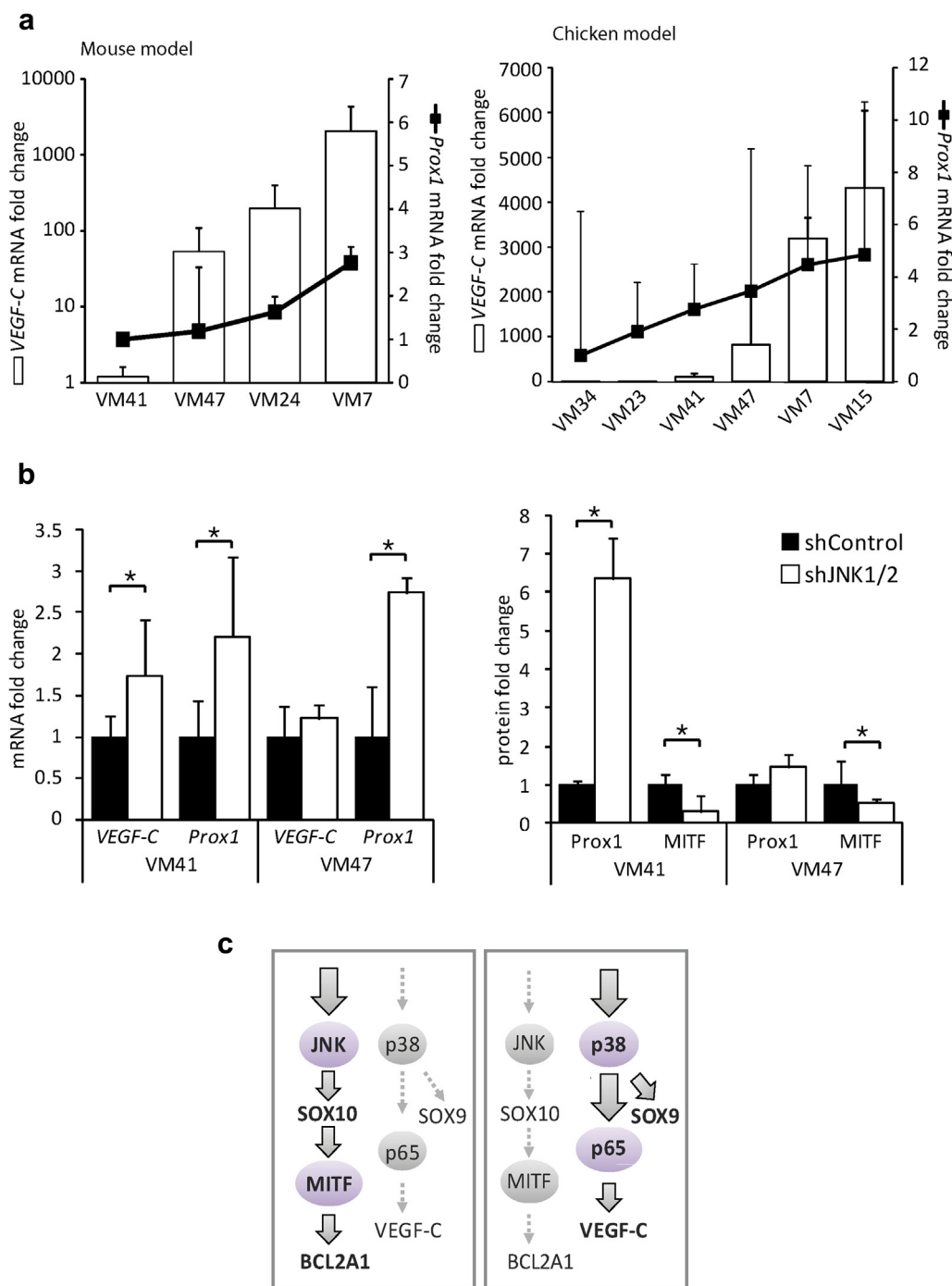
Figure 5. JNK activity determines VEGF-C expression and lymphangiogenesis in melanoma in vivo. (a) Xenograft mouse (left panel) and chicken CAM (right panel) model with indicated human melanoma cells. Human VEGF-C mRNA (left *y*-axis) and mouse or chicken Prox1 mRNA (right *y*-axis) was quantified by RT-PCR; n = 3/group, mean ± SD. (b) Xenograft mouse model with indicated melanoma cells carrying JNK1/2 knockdown (shJNK1/2) or control vector (shControl), harvested after 43 days. Human VEGF-C and mouse Prox1 mRNA was quantified by RT-PCR (left panel). Mouse Prox1 and human MITF protein expression determined by western blotting and quantified as Prox1/β-actin or MITF/β-actin ratios (right panel). VM41, n = 8/group; VM47, n = 4/group; *$P < 0.05$, mean ± SD. (c) Diagram of the proposed regulatory pathways for MITF and VEGF-C expression in human melanoma. CAM, chorioallantoic membrane; JNK, c-Jun N-terminal kinase; MITF, microphthalmia-associated transcription factor; VEGF-C, vascular endothelial growth factor C.

DISCUSSION

VEGF-C is the best studied and strongest lymphangiogenic growth factor (Alitalo and Detmar, 2012), and as expected, the lymphangiogenic potential of our melanoma cells directly correlates with VEGF-C levels. VEGF-D, another potent lymphangiogenic growth factor (Tammela et al., 2005), is poorly expressed in our melanoma cells and expression does not correlate with VEGF-C or MITF (data not shown). MITF is involved in melanocyte-specific pathway regulation (Mort et al., 2015). MITF expression levels determine the growth rate and invasive potential of melanoma; MITF[low] melanomas display a migratory and invasive phenotype (Carreira et al., 2006; Cheli et al., 2012; Hoek and Goding, 2010; Koludrovic and Davidson, 2013). Thus, low MITF expression associated with high levels of VEGF-C results in cells with high migratory potential combined with strong induction of lymphangiogenesis, thereby multiplying chances of metastasis. Here we modulate JNK/p38 pathway activities and create conditions recapitulating the melanoma phenotype switch in an experimental model. We show that high JNK activity results in high MITF levels and in a proliferative, but poorly migratory and lymphangiogenic phenotype, whereas high p38 activity results in low MITF and high VEGF-C expression, resulting in highly mobile

and lymphangiogenic phenotype. Using MITF and VEGF-C expression levels as surrogate markers for the respective JNK and p38 activities, we found a VEGF-C^{high}/MITF^{low} phenotype mostly in primary lesions of those patients that exhibited metastasis to sentinel nodes at the time of excision or shortly thereafter.

Our studies demonstrate that MITF is a downstream target of JNK. The knockdown decreases and upregulation of JNK increases MITF levels. Furthermore, by inhibiting the JNK downstream target c-Fos, MITF expression was reduced likewise. The link between JNK and MITF is strengthened by the fact that both are known regulators of cell proliferation and target the anti-apoptotic oncogene BCL2 (Deng et al., 2001; McGill et al., 2002). Accordingly, in shJNK1/2 cells, not only MITF but also BCL2A1 was significantly downregulated. Of note, in other cell types such as osteoclasts, p38 may increase MITF activity, albeit on a posttranslational level (Mansky et al., 2002).

The regulation of VEGF-C via JNK activity is more complex. On the basis of the JNK-IN-8-inhibitor effects, we initially assumed that JNK might act as a suppressor of VEGF-C expression, but overexpression of JNK1/2 did not alter VEGF-C expression. We also excluded the extracellular signal-regulated kinase pathway as being responsible for changes in VEGF-C and MITF expression, because inhibition of JNK in our cells did not lead to changes in p44/42 activity and cell lines with BRAF^{V600E} mutation did not show increased VEGF-C expression. Given the clear antipodal phosphorylation pattern of JNK and p38 in our cells, we considered a p38-dependent regulation of VEGF-C expression. p38 signaling is known to increase VEGF-C expression through NFκB activation in breast cancer cells (Tsai et al., 2003). This was reproducible in our melanoma cells. We found increased p38 and p65 phosphorylation in shJNK1/2 cells. Moreover, on silencing JNK, p65 bound more efficiently to oligonucleotides carrying the NFκB site within the VEGF-C promoter (Du et al., 2014) when compared with the controls.

The mutual interference between the JNK and p38 pathways has been described (Wagner and Nebreda, 2009). In our experiments, this interdependence between the JNK/p38 pathways does not appear to be an artifact of the JNK knockdown, because the basal phosphorylation levels of JNK or p38 in our cell lines concur with this pattern: high basal phosphorylation levels of JNK correlated with low p38 phosphorylation and vice versa, indicating that this is an intrinsic regulatory signal. The interdependence of JNK and p38 is mirrored by the fact that both may compete for proteins of the AP1 complex to form signaling-competent heterodimers; enhanced JNK signaling may reduce p38 signaling and vice versa (Karin, 1995). Interestingly, the c-Fos/AP1 inhibitor T-5224 inhibited expression of MITF and concomitantly augmented VEGF-C expression. Although the specificity of T-5224 for c-Fos is not well characterized, it is possible that T-5224 impairs the formation of JNK-induced c-Jun-c-Fos heterodimers and favors p38 signaling through increased availability of c-Jun for the formation of c-Jun-ATF2 (activating transcription factor 2) heterodimers. We have not directly addressed this issue, but in our melanoma cells c-Fos mRNA expression correlates positively with MITF and

negatively with VEGF-C, whereas ATF2 mRNA expression correlates negatively with MITF and positively with VEGF-C expression (Supplementary Figure S6 online). This negative relationship between ATF2 and MITF was previously described in melanocytes expressing transcriptionally inactive ATF2 resulting in increased MITF expression (Shah et al., 2010).

Another interesting aspect is that SOX10 expression follows MITF levels and SOX9 those of VEGF-C. For SOX10 and MITF, this is not unexpected as SOX10 transactivates MITF gene expression and both are markers of proliferative phenotype (Verfaillie et al., 2015). SOX9 is a p38 downstream target (Tew and Hardingham, 2006) that is upregulated on downregulation of SOX10 (Shakhova et al., 2015). We found the respective JNK and p38 activities responsible for two phenotypes of melanoma: JNK^{low}/p38^{high} activity results in a SOX9^{high}/VEGF-C^{high} phenotype, which is invasive and lymphangiogenic. In contrast, JNK^{high}/p38^{low} activity results in a MITF^{high}/SOX10^{high} phenotype, which is proliferative. This raises the question whether a therapeutic increase in JNK activity in advanced melanoma may switch cells into a proliferative, but poorly mobile and lymphangiogenic phenotype, which may then be less able to undergo hypoxia-induced mesenchymal transition and be better targeted by, for example, DNA alkylating agents. Nonetheless, using MITF and VEGF-C expression levels as surrogate markers for the respective JNK and p38 activities, we show that high VEGF-C and low MITF levels in primary lesions allow predicting metastasis. This conclusion is based on a retrospective analysis of a limited number of cases and requires confirmation in a prospective study, but underscores the relevance of the JNK and p38 for melanoma progression.

METHODS
Methods for cell culture, Western, ELISA, proliferation assay, cell cycle analysis, migration and invasion assays, spheroid sprouting assay, and immunofluorescence are described in Supplementary Materials online.

Microarrays analysis
mRNA expression patterns of 22 patient-derived melanoma cell lines were determined by Agilent.SingleColor.14850 (4 × 44K format) (Mathieu et al., 2012) and analyzed with GeneSpringGX software (Agilent Technologies, Santa Clara, CA) using default parameters (Guided Workflow). Samples were thresholded to 1, shifted to 75% percentile, and the baseline was set to medians of all samples. The normalized mRNA values, deposited under accession number GSE71122 at GEO/NCBI database (http://www.ncbi.nlm.nih.gov/geo/), were used in the Pearson correlation analysis with IBM SPSS Statistics 21 (Armonk, NY). For probe IDs see Supplementary Figure S1c.

The GEO/NCBI database was also used to correlate VEGF-C and MITF mRNA expression in 11 different studies encompassing 429 patients. Probes IDs were 209946_at for VEGF-C and 207233_s_at for MITF.

Antibodies and reagents
Antibodies were anti-phospho-JNK (#4668), anti-stress-activated protein kinase/JNK (#9258), anti-phospho-p38 (#4511), anti-p38 MAPK (clone D13E1, #8690), anti-phospho-p44/42 (#9101), anti-phospho-c-Jun (#3270), and anti-phospho-p65 (#3033) (all Cell

Signaling Technology, Danvers, MA). Anti-MITF (ab12039) (Abcam, Cambridge, UK), NCL-MITF (MITF-S) (Leica Biosystems, Wetzlar, Germany), anti-p65 (sc-109) (Santa Cruz, Dallas TX), anti-Prox1 (DP3501PX) (Acris, Herford, Germany), anti-β-actin (A2228), DAPI (D9542) (Sigma-Aldrich, St. Louis, MO), biotinylated secondary antibodies from Vector Laboratories (Burlingame, CA), and Alexa Fluor488 labeled secondary antibody (A11070) (Life Technologies, Thermo Fisher Scientific, Waltham, MA). For immunohistochemistry we used NCL-MITF (Leica Biosystems) and anti-VEGF-C (AF752) (R&D Systems, Minneapolis, MN).

Kinase inhibitors used were JNK-IN-8, NFκB-activation inhibitor 481406 (both Merc Millipore, Billerica, MA) and SB202190 (Sigma-Aldrich), and AP1/c-Fos inhibitor T-5224 was described earlier (Aikawa et al., 2008).

Immunohistochemistry

Melanoma metastases used in Figure 1d were from an unselected group of patients (primary tumors had a mean Breslow of 3 ± 2.2 mm). From paraffin blocks, tissue arrays were produced as published previously (Guinea-Viniegra et al., 2012). In brief, 0.5-mm punches were taken out of the paraffin-embedded melanoma metastasis by parallel viewing of hematoxylin and eosin stained sections, embedded into a new paraffin block and processed as described above.

Human primary melanoma tissue samples used in Figure 1e were from patients diagnosed between 2008 and 2010 and selected based on a Breslow of > 1 mm. Tissues were cut into 5 μm sections, deparaffinized and subjected to standard immunohistochemistry (Heinz et al., 2014). Slides were digitalized with ScanScope CS2 (Aperio Technologies, Vista, CA) and the stainings were quantified by a trained dermatopathologist blinded to the clinical status of the patient as exemplified in Figure 1c.

Real time PCR

RNA extracted with an RNeasy Mini kit (Qiagen, Hilden, Germany) was reverse transcribed to cDNA with a Revert Aid H First Strand cDNA kit (Life Technologies) using random hexamer primers. For RT-PCR, the TaqMan RT-PCR master mix and FAM primers (both Applied Biosystems, Foster City, CA) were used. Cycling parameters were 50 °C for 2 minutes, 95 °C for 10 minutes, followed by 40 cycles at 95 °C for 10 seconds and 60 °C for 1 minute. Glyceraldehyde-3-phosphate dehydrogenase (human or chicken) and β_2 microglobulin (mouse) were run as housekeeping genes. The mean Ct-value of the housekeeping gene was subtracted from the mean Ct-value of gene of interest (ΔCt). The ΔCt of "treatment" samples was subtracted from the ΔCt of control samples (ΔΔCt) and fold changes were calculated by the formula $2^{\wedge}(-\Delta\Delta Ct)$. RT-PCRs were ran on the StepOnePlus program and analyzed with the StepOnePlus v2.0 software (Applied Biosystems).

Chicken mRNA was quantified with the QuantiTect SYBR Green (Qiagen) reagent. Chicken Prox1 primers: forward 5′-GTCGCCGAA CCACCACTTGAAAA-3′, reverse 5′-CCACTTGATGAGCTGAGAG GT-3′; chicken glyceraldehyde-3-phosphate dehydrogenase primers: forward 5′-CCTGCTGCCTAGGGAAGG-3′, reverse 5′-CAGATCAGT TTCTATCAGCCTCT-3′ (Eurofins Genomics, Luxembourg).

Plasmid constructs, cloning, transfection, and viral infection

JNK1/2 silencing was done with shRNA constructs from S. Andreadis carrying the sequences: JNK1/2: AAAGAATGTCCTACCTTCT, JNK1: GGGCCTACAGAGAGCTAGTTCTTAT, JNK2: GCCAACTGTGAGG AATTATGTCGAA embedded in a second generation lentiviral

pLVTHM backbone coexpressing green fluorescent protein (GFP) (Lee et al., 2011). The packaging plasmid psPAX2 and the envelope plasmid pMD2.G (Addgene plasmids #12260 and #12259, from Didier Trono) were cotransfected using Lipofectamine2000 (Invitrogen, Carlsbad, CA) into 293T-cells. The GFP-pLVTHM vector was used as a negative control (Addgene #12247). Media containing lentiviral particles were collected 48 hours after infection and added to melanoma cells in 2/1 ratio with RPMI and 6 μg/ml Polybrene (Santa Cruz). Cells were then sorted for GFP expression.

Plasmids for JNK1/2 overexpression (JNK1a1/1b1 and JNK2a1/2b1 pCDNA3-Flag) were from Roger Davis (Addgene #13753, #13754, #13756, and #13798), and the MITF-Flag-pCMV plasmid was from J. Vachtenheim, Charles University Prague. Transient overexpression was achieved by using Lipofectamine2000; cells were analyzed for mRNA and protein expression 72 hours later. The MITF-Flag insert was cut out of the pCMV backbone and cloned into retroviral pBABE-puro backbone (Hartmut Land, Jay Morgenstern, and Bob Weinberg, Addgene #1764). Retroviral particles were collected from 293T-cells expressing the MITF-pBABE plasmid, together with pUMVC and pCMV-VSV-G (Bob Weinberg, Addgene #8449 and #8454), as described above. The SOX9-pcDNA-5′-UT used for transient SOX9 overexpression was from Benoit de Crombrugghe, University of Texas, USA. The plasmid used for overexpression of VEGF-C was described earlier (Niederleithner et al., 2012). P65-pEGFP-C1 used for the ABCD assay was described earlier (Schmid et al., 2000). pBABE-puro-hTERT-HA was from Bob Weinberg, Addgene #1772.

ABCD assays

The ABCD assay was used to determine p65 DNA binding activity using oligonucleotides with an NFκB consensus sequence and oligonucleotides with a stretch of VEGF-C promoter sequence including the putative NFκB site (Du et al., 2014). The sequences of 5′ biotinylated NFκB consensus were: forward 5′-GGGAAA TTCCCGGAAATTCCCGGAAATTCCCGGAAATTCC-3′, reverse 5′-GGAATTTCCGGGAATTTCCGGGAATTTCCGGGAATTTCCC-3′. The sequences of 5′ biotinylated VEGF-C promoter sequence were: forward 5′-GAGGGAAACGGGGAGCTCCAGGGAGGAGGGAA ACGGGGAGCTCCAGGGAGGAGGGAAACGGGGAGCTCCAGG GA-3′, reverse 5′-TCCCTGGAGCTCCCCGTTTCCCTCCTCCCTGG AGCTCCCCGTTTCCCTCCTCCC TGGAGCTCCCCGTTTCCCTC-3′. The sequences of 5′ biotinylated mutant VEGF-C promoter sequence were: forward 5′-GAGGGAAACGGTTCGCTCCAGGGAGGAGGG AAACGGTTCGCTCCAGGGAGGAGGGAAACGGTTCGCTCCAGG GAG-3′, reverse 5′-CTCC CTGGAGCGAACCGTTTCCCTCCTCCCTG GAGCGAACCGTTTCCCTCCTCCCTGGAGCGAACCGTTTCCCTC-3′. The protocol was described earlier (Sahin et al., 2014). Briefly, cells were lysed and incubated in Buffer H containing 50 mM KCl and oligonucleotides. Specificity of the oligonucleotides was assessed using nonbiotinylated oligonucleotides (cold control) at 10-fold excess and oligonucleotides with a mutated NFκB site for the VEGF-C promoter sequence.

In vivo experiments

The mouse xenograft model was described earlier (Loewe et al., 2006; Niederleithner et al., 2012). Briefly, melanoma cells (2×10^6 cells/mouse) were injected intradermally to the flanks of 8 weeks' female hairless severe combined immunodeficient mice (Crl:SHO-PrkdcscidHrhr, Charles River Laboratories, Wilmington, MA). Tumors were measured with a caliper and the volume was calculated with the formula $V = (\pi/6) \times (length) \times (width)^2$. The

tumors were excised at sizes of 400 mm^3. The tumors from melanoma cell lines expressing either shControl or shJNK1/2 plasmids were excised after 43 days because of growth retardation of the shJNK1/2 tumors.

Eggs were from white Leghorn chickens (regional farmer, Gloggnitz, Austria). Melanoma cells (0.5×10^6) in RPMI (without supplements) were placed onto the chorioallantoic membrane of 10-day-old embryos. Five days later, visible tumors with a diameter of approximately 5 mm that had formed (sizes indistinguishable between groups) were excised, lysed in RLT buffer (Qiagen) with 1% β-ME, mRNA extracted, and quantified by RT-PCR.

Statistics

All data are results of at least three independent experiments performed at least twice; data are expressed as mean ± SD. When comparing two groups, significance was assessed by two-sided Student's *t*-test. For comparison of more than two groups, one-way ANOVA followed by Tukey's honestly significant difference test was used. For the statistical analysis of immunohistochemistry stainings in correlation with metastasis (Figure 1e), the Mann-Whitney *U*-test was performed. The correlations between two variables were assessed as the Pearson product-moment correlation coefficient. All statistical analysis was done with IBM SPSS Statistics 21.

Study approval

All in vivo experiments followed the Declaration of Helsinki protocols. Retrieval of human melanoma sections for immunohistology was according to ethics committee permission 405/2006 and extension 075/09/2014 after written informed consent. All animal experiments were approved and executed according to the guidelines of the animal care and use committee of Medical University of Vienna, ethics permissions BMBWK-66.009/0192-II/3b/2012 and BMBWK-66.009/0211-WF/II/3b/2014.

SUPPLEMENTARY MATERIAL

Supplementary material is linked to the online version of the paper at www.jidonline.org, and at http://dx.doi.org/10.1016/j.jid.2016.01.020.

REFERENCES

Aikawa Y, Morimoto K, Yamamoto T, Chaki H, Hashiramoto A, Narita H, et al. Treatment of arthritis with a selective inhibitor of c-Fos/activator protein-1. Nat Biotechnol 2008;26:817—23.

Alitalo A, Detmar M. Interaction of tumor cells and lymphatic vessels in cancer progression. Oncogene 2012;31:4499—508.

Balch CM, Gershenwald JE, Soong SJ, Thompson JF, Atkins MB, Byrd DR, et al. Final version of 2009 AJCC melanoma staging and classification. J Clin Oncol 2009;27:6199—206.

Bracher A, Cardona AS, Tauber S, Fink AM, Steiner A, Pehamberger H, et al. Epidermal growth factor facilitates melanoma lymph node metastasis by influencing tumor lymphangiogenesis. J Invest Dermatol 2013;133:230—8.

Carreira S, Goodall J, Denat L, Rodriguez M, Nuciforo P, Hoek KS, et al. Mitf regulation of Dia1 controls melanoma proliferation and invasiveness. Genes Dev 2006;20:3426—39.

Cheli Y, Giuliano S, Fenouille N, Allegra M, Hofman V, Hofman P, et al. Hypoxia and MITF control metastatic behaviour in mouse and human melanoma cells. Oncogene 2012;31:2461—70.

Chen JC, Chang YW, Hong CC, Yu YH, Su JL. The role of the VEGF-C/VEGFRs axis in tumor progression and therapy. Int J Mol Sci 2013;14:88—107.

Cianfarani F, Mastroeni S, Odorisio T, Passarelli F, Cattani C, Mannooranparampil TJ, et al. Expression of vascular endothelial growth factor-C in primary cutaneous melanoma predicts sentinel lymph node positivity. J Cutan Pathol 2012;39:826—34.

Dadras SS, Paul T, Bertoncini J, Brown LF, Muzikansky A, Jackson DG, et al. Tumor lymphangiogenesis. Am J Pathol 2003;162:1951—60.

Deng X, Xiao L, Lang W, Gao F, Ruvolo P, May WS. Novel role for JNK as a stress-activated Bcl2 kinase. J Biol Chem 2001;276:23681—8.

Doeden K, Ma Z, Narasimhan B, Swetter SM, Detmar M, Dadras SS. Lymphatic invasion in cutaneous melanoma is associated with sentinel lymph node metastasis. J Cutan Pathol 2009;36:772—80.

Du Q, Jiang L, Wang X, Wang M, She F, Chen Y, et al. Tumor necrosis factor-α promotes the lymphangiogenesis of gallbladder carcinoma of vascular endothelial growth factor-C. Cancer Sci 2014;105:1261—71.

Guinea-Viniegra J, Zenz R, Scheuch H, Jiménez M, Bakiri L, Petzelbauer P, et al. Differentiation-induced skin cancer suppression by FOS, p53, and TACE/ADAM17. J Clin Invest 2012;122(8):2898—910.

Hartman ML, Czyz M. MITF in melanoma: mechanisms behind its expression and activity. Cell Mol Life Sci 2015;72:1249—60.

Heinz M, Niederleithner H, Puujalka E, Soler-Cardona A, Grusch M, Pehamberger H, et al. Activin A is anti-lymphangiogenic in a melanoma mouse model. J Invest Dermatol 2014;135:212—21.

Hoek KS, Eichhoff OM, Schlegel NC, Döbbeling U, Kobert N, Schaerer L, et al. In vivo switching of human melanoma cells between proliferative and invasive states. Cancer Res 2008a;68:650—6.

Hoek KS, Goding CR. Cancer stem cells versus phenotype-switching in melanoma. Pigment Cell Melanoma Res 2010;23:746—59.

Hoek KS, Schlegel NC, Eichhoff OM, Widmer DS, Praetorius C, Einarsson SO, et al. Novel MITF targets identified using a two-step DNA microarray strategy. Pigment Cell Melanoma Res 2008b;21:665—76.

Howlin J, Cirenajwis H, Lettiero B, Staaf J, Lauss M, Saal L, et al. Loss of CITED1, an MITF regulator, drives a phenotype switch in vitro and can predict clinical outcome in primary melanoma tumours. PeerJ 2015;3:e788.

Jeltsch M, Kaipainen A, Joukov V, Meng X, Lakso M, Rauvala H, et al. Hyperplasia of lymphatic vessels in VEGF-C transgenic mice. Science 1997;276:1423—5.

Karin M. The regulaion of AP-1 activity by mitogen-activated protein kinases. J Biol Chem 1995;270:16483—6.

Koludrovic D, Davidson I. MITF, the Janus transcription factor of melanoma. Futur Oncol 2013;9:235—44.

Lee M-H, Padmashali R, Andreadis ST. JNK1 is required for lentivirus entry and gene transfer. J Virol 2011;85:2657—65.

Loewe R, Valero T, Kremling S, Pratscher B, Kunstfeld R, Pehamberger H, et al. Dimethylfumarate impairs melanoma growth and metastasis. Cancer Res 2006;66:11888—96.

Luangdilok S, Box C, Harrington K, Rhŷs-Evans P, Eccles S. MAPK and PI3K signalling differentially regulate angiogenic and lymphangiogenic cytokine secretion in squamous cell carcinoma of the head and neck. Eur J Cancer 2011;47:520—9.

Mansky KC, Sankar U, Han J, Ostrowski MC. Microphthalmia transcription factor is a target of the p38 MAPK pathway in response to receptor activator of NF-κB ligand signaling. J Biol Chem 2002;277:11077—83.

Mathieu V, Pirker C, Schmidt WM, Spiegl-Kreinecker S, Lötsch D, Heffeter P, et al. Aggressiveness of human melanoma xenograft models is promoted by aneuploidy-driven gene expression deregulation. Oncotarget 2012;3:399—413.

Matsui J, Funahashi Y, Uenaka T, Watanabe T, Tsuruoka A, Asada M. Multikinase inhibitor E7080 suppresses lymph node and lung metastases of human mammary breast tumor MDA-MB-231 via inhibition of vascular endothelial growth factor-receptor (VEGF-R) 2 and VEGF-R3 kinase. Clin Cancer Res 2008;14:5459—65.

McGill GG, Horstmann M, Widlund HR, Du J, Motyckova G, Nishimura EK, et al. Bcl2 regulation by the melanocyte master regulator

Mitf modulates lineage survival and melanoma cell viability. Cell 2002;109:707—18.

Mort RL, Jackson IJ, Patton EE. The melanocyte lineage in development and disease. Development 2015;142:620—32.

Niederleithner H, Heinz M, Tauber S, Bilban M, Pehamberger H, Sonderegger S, et al. Wnt1 is anti-lymphangiogenic in a melanoma mouse model. J Invest Dermatol 2012;132:2235—44.

Pastushenko I, Vermeulen PB, Carapeto FJ, Van Den Eynden G, Rutten A, Ara M, et al. Blood microvessel density, lymphatic microvessel density and lymphatic invasion in predicting melanoma metastases: systematic review and meta-analysis. Br J Dermatol 2014;170:66—77.

Podgrabinska S, Skobe M. Role of lymphatic vasculature in regional and distant metastases. Microvasc Res 2014;95:46—52.

Roberts N, Kloos B, Cassella M, Podgrabinska S, Persaud K, Wu Y, et al. In-hibition of VEGFR-3 activation with the antagonistic antibody more potently suppresses lymph node and distant metastases than inactivation of VEGFR-2. Cancer Res 2006;66:2650—7.

Sahin E, Haubenwallner S, Kuttke M, Kollmann I, Halfmann A, Dohnal AB, et al. Macrophage PTEN regulates expression and secretion of arginase I modulating innate and adaptive immune responses. J Immunol 2014;193:1717—27.

Schietroma C, Cianfarani F, Lacal PM, Odorisio T, Orecchia A, Kanitakis J, et al. Vascular endothelial growth factor-C expression correlates with lymph node localization of human melanoma metastases. Cancer 2003;98:789—97.

Schmid JA, Birbach A, Hofer-Warbinek R, Pengg M, Burner U, Furtmüller PG, et al. Dynamics of NF kappa B and Ikappa Balpha studied with green fluorescent protein (GFP) fusion proteins. Investigation of GFP-p65 binding to DNA by fluorescence resonance energy transfer. J Biol Chem 2000;275:17035—42.

Shah M, Bhoumik A, Goel V, Dewing A, Breitwieser W, Kluger H, et al. A role for ATF2 in regulating MITF and melanoma development. PLoS Genet 2010;6:1—21.

Shakhova O, Cheng P, Mishra PJ, Zingg D, Schaefer SM, Debbache J, et al. Antagonistic cross-regulation between Sox9 and Sox10 controls an anti-tumorigenic program in melanoma. PLoS Genet 2015;11:e1004877.

Shields JD, Borsetti M, Rigby H, Harper SJ, Mortimer PS, Levick JR, et al. Lymphatic density and metastatic spread in human malignant melanoma. Br J Cancer 2004;90:693—700.

Sosa MS, Parikh F, Maia AG, Estrada Y, Bosch A, Bragado P, et al. NR2F1 controls tumour cell dormancy via SOX9- and RARβ-driven quiescence programmes. Nat Commun 2014;30:6170.

Stacker SA, Williams SP, Karnezis T, Shayan R, Fox SB, Achen MG. Lym-phangiogenesis and lymphatic vessel remodelling in cancer. Nat Rev Cancer 2014;14:159—72.

Swoboda A, Schanab O, Tauber S, Bilban M, Berger W, Petzelbauer P, et al. MET expression in melanoma correlates with a lymphangiogenic pheno-type. Hum Mol Genet 2012;21:3387—96.

Tammela T, Enholm B, Alitalo K, Paavonen K. The biology of vascular endothelial growth factors. Cardiovasc Res 2005;65:550—63.

Tew SR, Hardingham TE. Regulation of SOX9 mRNA in human articular chondrocytes involving p38 MAPK activation and mRNA stabilization. J Biol Chem 2006;281:39471—9.

Tsai P-W, Shiah S-G, Lin M-T, Wu C-W, Kuo M-L. Up-regulation of vascular endothelial growth factor C in breast cancer cells by heregulin-beta 1. A critical role of p38/nuclear factor-kappa B signaling pathway. J Biol Chem 2003;278:5750—9.

Verfaillie A, Imrichova H, Atak ZK, Dewaele M, Rambow F, Hulselmans G, et al. Decoding the regulatory landscape of melanoma reveals TEADS as regulators of the invasive cell state. Nat Commun 2015;6:6683.

Wagner EF, Nebreda AR. Signal integration by JNK and p38 MAPK pathways in cancer development. Nat Rev Cancer 2009;9:537—49.